Rotating Waves as a Stall Inception Indication in Axial Compressors

V. H. GARNIER, A. H. EPSTEIN, E. M. GREITZER
Gas Turbine Laboratory
Massachusetts Institute of Technology
Cambridge, MA 02139

ABSTRACT

Stall inception has been studied in two low speed compressors (a single-stage and a three-stage) and in a high speed three-stage compressor, using temporally and spatially resolved measurements. In all three machines, rotating stall was preceded by a period in which small amplitude waves were observed travelling around the circumference of the machine at a speed slightly less than the fully developed rotating stall cell speed. The waves evolved smoothly into rotating stall without sharp changes in phase or amplitude, implying that, in the machines tested, the prestall waves and the fully developed rotating stall are two stages of the same phenomenon. The growth rate of these disturbances was in accord with that predicted by current analytical models. The prestall waves were observed both with uniform and with distorted inflow, but were most readily discerned with uniform inflow. Engineering uses and limitations of these waves are discussed.

NOMENCLATURE

a_k, b_k	Fourier components of disturbance velocity potential
c_k	Fourier component of axial velocity disturbance
k	harmonic number
δP	pressure perturbation
R	compressor midspan radius
u	axial velocity perturbation (see Appendix)
U	rotor speed at midspan
η	non-dimensional axial coordinate; η = axial distance/R
θ	circumferential coordinate
λ, μ	compressor inertia parameters
ξ	non-dimensional time; ξ = (time·U)/R
σ	non-dimensional damping ratio (see Eq. (1))
ϕ	compressor flow coefficient; ϕ = axial velocity/U
Φ	non-dimensional compressor velocity potential
ψ	compressor pressure rise; $P_{exit} - Pt_{inlet} / \frac{1}{2} \rho U^2$
ω	non-dimensional frequency; ω = frequency·(U/R)

INTRODUCTION

Axial compressors are subject to two distinct aerodynamic instabilities, rotating stall and surge, which can severely limit compressor performance. Rotating stall is characterized by a wave travelling about the circumference of the machine, surge by a basically one-dimensional fluctuation in mass flow through the machine. Whether these phenomena are viewed as distinct (rotating stall is local to the blade rows and dependent only on the compressor, while surge involves the entire pumping system -- compressor, ducting, plenums, and throttle) or as related (both are eigenmodes of the compression system with surge being the zeroth order mode), they cannot be tolerated during compressor operation. Both rotating stall and surge reduce the pressure rise in the machine, cause rapid heating of the blades, and can induce severe mechanical distress.

The instabilities are commonly avoided by operating the compressor at a reduced pressure rise so as to leave a safety margin, the so-called "surge margin", between the operating point of the compressor and the point at which the machine surges. The requirement for surge margin reduces the available operating pressure rise from a given machine and often reduces the operating efficiency as well. Reduction of surge margin can then translate directly into compressor weight and efficiency improvement so that there is practical incentive to reducing the surge margin required. In the high speed compressors common to aircraft engines, rotating stall and surge are closely coupled. As the machine moves along a constant speed operating line toward lower mass flow (Fig. 1), it generally first encounters rotating stall, which then (loosely) "triggers" the surge, often after only one or two rotor revolutions. Thus, surge and stall must both be considered; the compressor surge line could really be considered the rotating stall line, and the surge margin as stall margin.

We are aware of several alternate approaches under investigation for reducing the stall margin required. They can be considered to fall into one of two categories -- those based on moving the operating point close to the stall line in situations when surge and stall do not threaten, and those based on moving the surge line itself and thus increasing the stable range of the compressor. Efforts in the former category include: (a) a real-time assessment of the stall margin by correlation of the instantaneous aircraft flight parameters with the measured compressor stall behavior; and (b) stall avoidance in which the control system detects rotating stall and then quickly moves the compressor operating point away from stall.

Dynamic compressor stabilization is based on an alternate approach. Here, the stall point is moved to lower mass flows by active feedback control. This scheme, and stall avoidance also, rely on the use of real-time measurements within the compressor to assess the machine stability. Clearly, the earlier a control system can detect a stall or even an incipient stall, the more effective (and less demanding) the control becomes.

This paper describes an experimental study of the rotating stall inception and growth process in three axial compressors. Its goals were both to illuminate the manner in which stall cells are born and
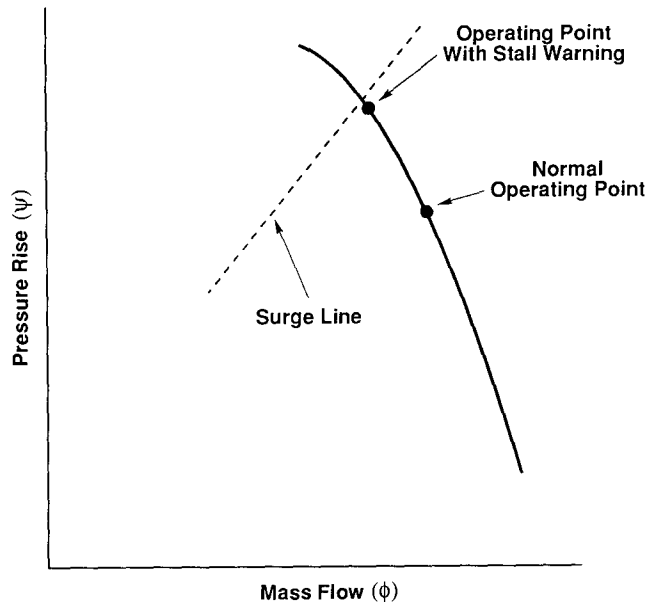
Fig. 1:   Compressor performance is characterized by the constant speed line shown (solid line). The compressor cannot be safely operated to the left of the surge line.

develop, as well as to establish, as suggested by theory, whether real-time information can be extracted from the compressor which would warn of an impending stall before the stall actually developed. This stall warning or "precursor" could have significant practical benefit if the warning is sufficiently in advance of the stall so as to permit time for control system response. The longer the warning, the greater the potential utility.

In the following sections, we review the relevant theoretical background on rotating stall development, describe the experimental arrangement, present data for three compressors under a variety of operating conditions, and finally comment on the generality of these findings and their usefulness.

BACKGROUND

A large amount of experimental data taken over the last twenty years shows that, if measured at a single point in the compressor, rotating stall is seen as a sudden event with a growth period on the order of the stall cell period. Stall detection schemes based on this sort of measurement have thus not been successful in providing appreciable warning time. During the same period, however, a theoretical basis for the description of rotating stall has arisen based on the understanding of rotating stall as one class of the natural instabilities of the compression system. At its current state of development (e.g., Moore and Greitzer, 1986), the model describes the time evolution of surge and rotating stall in a compressor treated mathematically as a two-dimensional incompressible device (i.e. large hub-to-tip ratio), with three-dimensional phenomena represented only through empirical inputs. The results of a prediction by this model for a representative three-stage compressor (Fig. 2) show an instability evolving as a small amplitude wave in axial velocity which grows as it travels around the circumference of the compressor until, through nonlinear interaction it causes a large amplitude disturbance in annulus average axial velocity (surge). This type of model provides the background for the present work.

As shown in the appendix, we can describe the stability of a compressor in terms of the time evolution of an asymmetric perturbation of the velocity potential, Φ, namely

$$\Phi = \sum_{|k| \neq 0} b_k \left\{ e^{|k|\eta - \sigma_k \xi} \right\} \left\{ e^{i(k\theta - \omega_k \xi)} \right\} \tag{1}$$

Each Fourier mode (k) is the product of two exponentials. The term $\exp(i[k\theta - \omega_k \xi])$ represents a travelling wave function of circumferential position (θ) and time (ξ); ω_k is the wave frequency. The term $\exp(|k|\eta - \sigma_k \xi)$ gives the dependence of the wave on axial position (η) and time; σ_k is the damping of the wave. Equation (1) can be viewed as analogous to the behavior of an oscillator rotating about the circumference of the compressor. The growth of the wave (i.e. the stability of the compressor) is determined by the instantaneous damping σ. When the damping is negative, oscillations grow and the flow in the compressor is unstable. Active control schemes aim to increase this damping. Here we make use of Eq. (1) in designing an experiment to detect the rotating waves and measure the instantaneous stability of the compressor.

McDougall (1988, 1989) was the first person known to the authors to have made measurements of these rotating waves. Examining a single-stage, low speed compressor, he found small disturbances rotating about the machine just prior to the onset of stall, in qualitative accord with the above theory. He included a good summary of previous experimental work.

To explore the use of the travelling waves as a stall precursor or warning, we pose the following questions:
- Do prestall waves exist in most (many, all) compressors?
- At what rate do these waves grow? How long do they persist?
- At what rate do they travel?
- How can they be observed?
- How is this behavior affected by inlet distortion and mass flow transients?
- Do high speed (compressible) machines behave similarly?

In sum, these questions address both the basic assumptions inherent in the Moore/Greitzer model and its utility in providing real-time warning of an impending compressor stall. In the following, we experimentally examine these issues.

EXPERIMENTAL APPARATUS

Prestall behavior of three compressors was examined -- two low speed and one high speed machine. The low speed, single-stage compressor consisted of IGV's, rotor, and stator. It is described in more detail by Johnson (1987) and Lee (1988). The low speed, three-stage compressor is described by Gamache (1986, 1990) and Lavrich (1988). Non-dimensional inlet total to exit static pressure compressor characteristics are shown for the two machines in Fig. 3. Both low speed compressors were operated at tip speeds below 100 m/s, so that compressibility effects were negligible. The high speed, three-stage compressor is a modern experimental design run at Pratt & Whitney Div., United Technologies Corp. This machine was equipped with fast-acting bleed valves which quickly moved the operating point away from stall when it occurred to prevent
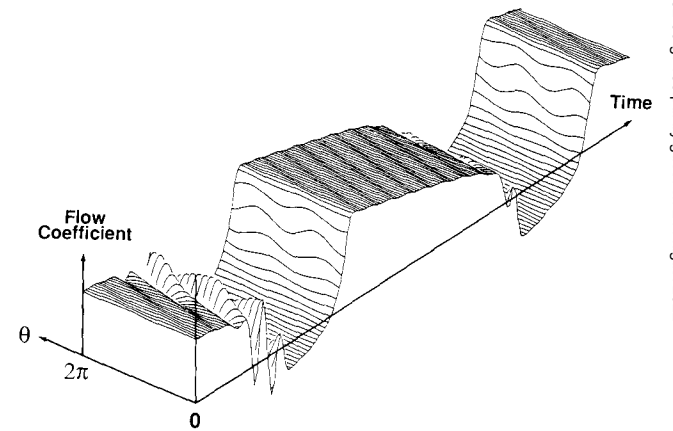

Fig. 2:   The time evolution of the non-dimensional axial velocity (C_x/U) distribution about the circumference ($0 \leq \theta \leq 2\pi$) of a three-stage compressor during compression system instability. Mean level of C_x/U prior to instability is 0.5.

2

mechanical damage. Experiments on that machine were conducted by Pratt & Whitney personnel and the raw data provided to the authors.

INSTRUMENTATION

All the compressors were outfitted with standard time-averaged instrumentation to provide the steady state operating characteristics of the machines. Time-resolved instrumentation consisted of hot wire anemometers in the low speed compressors (oriented so as to measure axial velocity), and wall-mounted, high response, static pressure transducers in the high speed compressor. The high speed machine had eight transducers mounted about the circumference at each of four axial stations. The low speed machines had either eight hot wires at a time at one axial station or three rows of four mounted at various stations. The low speed data was digitized in real time (with suitable low pass anti-aliasing filters), while the high speed data was first recorded on analog magnetic tape. All data was d.c. coupled.

The hot wires were calibrated in place prior to each test to a velocity accuracy of ±3%. The net resolution of the anemometers was 0.8% of the average prestall axial velocity. The pressure transducers in the high speed experiment were calibrated by Pratt & Whitney personnel. One pressure transducer had significantly less amplitude than all its neighbors so that its gain was raised in post-test processing to yield the same level of RMS fluctuations.
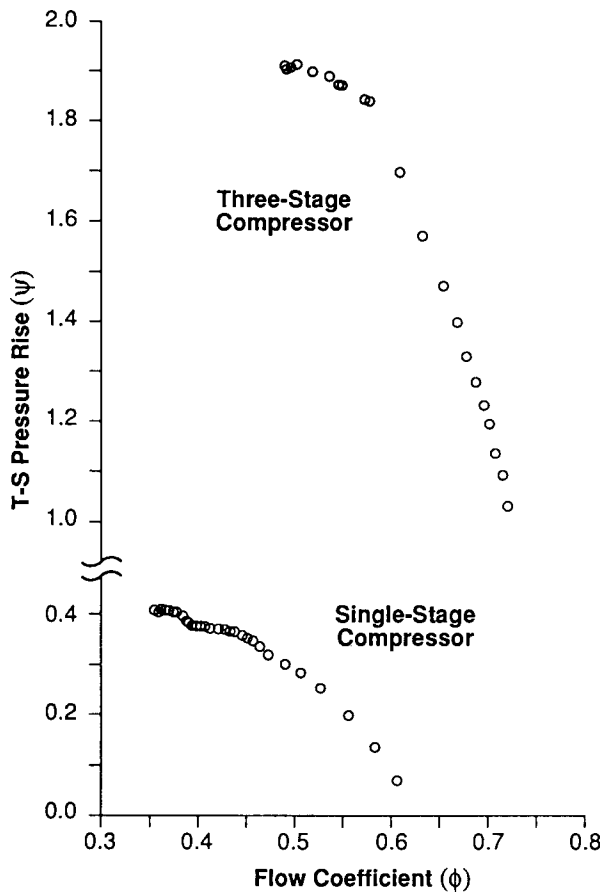
SIGNAL PROCESSING AND PROBE PLACEMENT CONSIDERATIONS

Experiments were conducted to look for small amplitude travelling waves whose spatial and temporal structure was important. Probe placement and signal processing were therefore carefully considered. Also, because the measurements in both time and space were discrete, aliasing was of concern in both dimensions.

Probe number was determined by the number of spatial harmonics (N) to be examined. 2N+1 measurement points are required about the circumference at each axial station. Eight were used in most cases, providing definition of the first three spatial harmonics. We expected most of the energy in the lowest order modes but were concerned about aliasing of the higher order modes and blade passing phenomena. Since small upstream disturbances due to the compressor are irrotational, they decay exponentially with upstream distance. Thus, the first measurements were made one-half compressor radius upstream so that high order (short length scale) disturbances would be filtered out fluid dynamically. These disturbances appeared not to be a problem and measurements were subsequently made throughout the compressors.

We expect the waves to travel about the circumference at close to the rotating stall frequency, 20-50% of rotor shaft speed. Thus, the data was digitally band-pass filtered in the computer, with a passband 0.1 to 1.2 times rotor shaft frequency. These frequencies were determined by trial and error comparison to the unfiltered data.

The filtered time histories of the individual sensors can be used to calculate the modal information by taking a discrete Fourier transform in space about the circumference of the compressor at each point in time. Given N measurements about the machine, the complex Fourier coefficients for each mode k are given by

$$C_k = \frac{1}{N} \sum_{n=0}^{N-1} V_n \exp\left[-\frac{2ikn\pi}{N}\right] \qquad (2)$$

Fig. 3: Compressor characteristics of the two low speed compressors examined in this study.
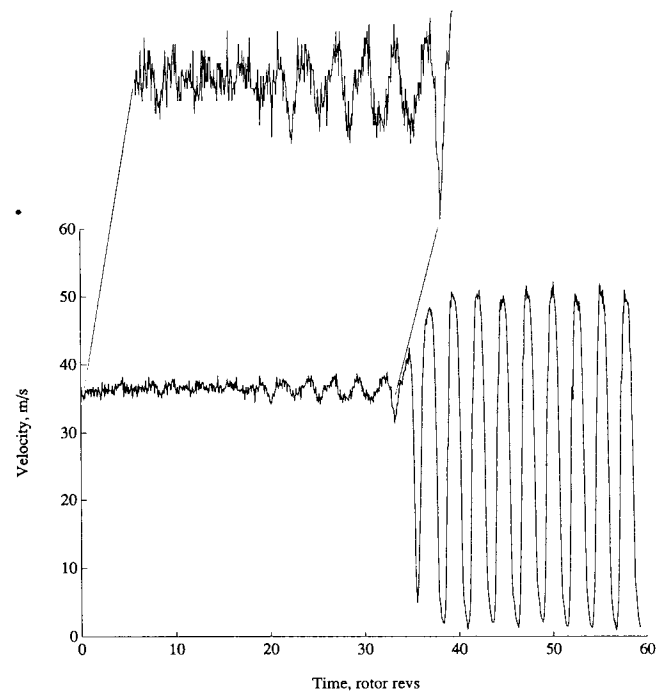

Fig. 4: Time history of axial velocity from a single hot wire positioned upstream of the single-stage compressor. The machine is in rotating stall after a time of 35 rotor revolutions.

3

bar

Downloaded from http://asmedigitalcollection.asme.org/GT/proceedings-pdf/GT1990/79047/V001T01A052/4216296/v001t01a052-90-gt-156.pdf by guest on 21 August 2022

where V_n is the measured axial velocity at angular position n. For most measurements described herein, eight sensors were used so that N = 8, -3 ≤ k ≤ 4, and, since V_n is real, C_k and C_{-k} are complex conjugates. The Fourier coefficients contain all the information on the wave position and amplitude as a function of time.

LOW SPEED COMPRESSOR EXPERIMENTS

The low speed single-stage and three-stage compressors were used to explore the nature of the stall initiation process and the prestall travelling wave behavior, examine alternate sensor placements, establish the travelling wave statistical behavior, and determine the influence of inlet distortion and throttle (mass flow) transients.

Quasi-Steady Stalling Behavior

During these experiments, the compressor operation was first stabilized very close to stall (within 0.005 in flow coefficient from the stall point in Fig. 3) and then the throttle closed very slowly so that machine would stall within 10 to 20 seconds. Data was taken during this entire period from the eight hot wires about the compressor annulus. Unless otherwise specified, the hot wires were positioned 0.5 compressor radii upstream of the IGV's.

Figure 4 shows the time history of the axial velocity as measured by a single sensor during the stalling transient. Here, time equal to zero has been defined, somewhat arbitrarily, as the time at which the velocity non-uniformity has grown to 50% of the fully stalled maximum value. The period of a rotor revolution is used as the unit of time since this is a characteristic time scale for the phenomena. As can be seen, the prestall fluctuations have a small amplitude compared to the rotating stall itself, during which the velocity fluctuations are greater than 100% of the prestall mean velocity. The time history of all eight sensors about the circumference is shown in Fig. 5 on a magnified scale, and regular disturbances can be observed here for a considerable time before the stall. The amplitude of the first Fourier component (the modulus of C_1), calculated from this data with Eq. (2), is shown in Fig. 6. This is a measure of the strength of the first mode of the rotating wave. Although small compared to the amplitude during fully developed rotating stall (t > 0), it is non-zero for a long period (90 revs) before the stall. The argument of C_1 is the phase angle of the travelling wave, and this is shown in Fig. 7 along with the phase of the second harmonic (arg C_2). The slopes of these lines are the speeds at which the harmonics of the waves travel around the compressor annulus (the annulus has been unwrapped in the figure so that 2π radians is one trip around). This coarse scale is used deliberately to show the overall trend. The

Fig. 6: Amplitude of the first Fourier harmonic ($|C_1|$) of the data in Fig. 5.

key point from Fig. 7 is that phase speed of the first harmonic of the travelling waves is essentially constant and readily discernible for almost 90 rotor revolutions before the stall. There is a small shift in wave speed at the stall point, from 0.35 rotor speed before the stall to 0.38 rotor speed with fully developed stall. The curve marked "second harmonic" shows that, for this experiment, the second harmonic signal is too weak (i.e. the signal-to-noise ratio is too small with the instrumentation used) to give useful information.

A three-dimensional representation of the C_1 component during the last 20 revs before stall is shown in Fig. 8 in a format similar to that of the calculation shown in Fig. 2. The wave nature of the disturbance in this machine is evident.

The amplitude of the oscillations in the compressor flowfield (in this case the travelling waves about the circumference) reflects not only the operating point but also the level of disturbances in the system (the forcing). Near the neutral stability point (damping, σ, close to zero), the flowfield should behave like a narrow band
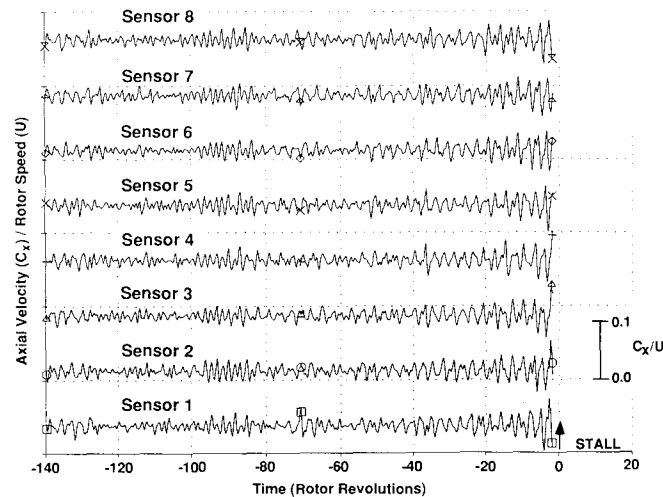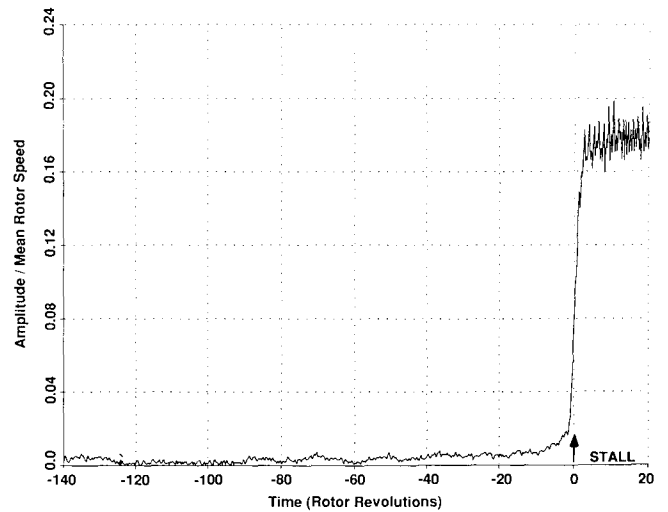

Fig. 5: Time history of axial velocity before stall as measured by 8 hot wires equally spaced about the circumference 0.4 compressor radii upstream of the IGV's.
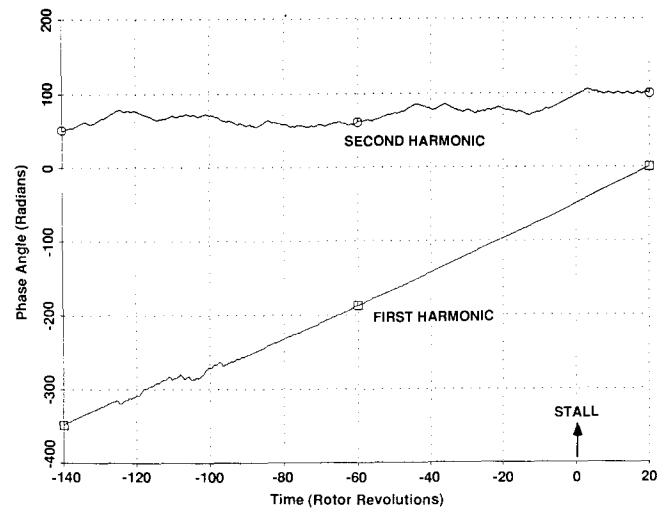

Fig. 7: The time history of the phase of the first and second Fourier coefficients measured upstream of the low speed, three-stage compressor.
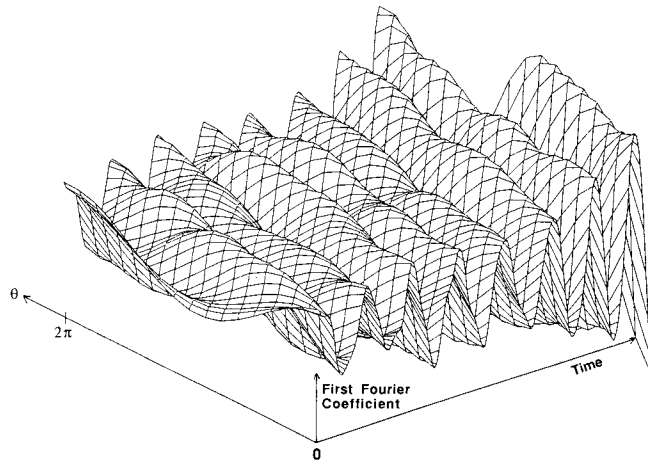
4

Fig. 8: Measured first harmonic behavior in a format comparable to that of Fig. 2.

system. Re-examining Fig. 7 we see that there is a stretch of constant phase speed between -140 and -125 revs, followed by a period of ill-defined speed to -95 revs, and then finally constant phase speed until stall at 0. In the context of the model, we interpret this to imply that the damping of the compressors (σ) is very close to zero, so that the travelling waves are very lightly damped. They can grow and then decay, depending upon the level of external disturbances. Thus, we might expect to see some test-to-test variation in the time during which the prestall waves propagate strongly enough to be evident. This was examined by carrying out nine tests on the three-stage compressor under nominally identical conditions. The mean prestall period of constant wave propagation was approximately 60 rotor revolutions with a high of 250 and a low of 30. (In all cases, the wave speed was 35% of rotor speed before stall and 38% during stall.) There is thus considerable statistical variation in the time during which the prestall waves were tracked. We have not characterized the source of these variations; they may be related to low amplitude external disturbances (noise) convected into the compressor inlet. Overall, these data establish that rotating stall starts as a small amplitude travelling wave in the two low speed compressors studied.
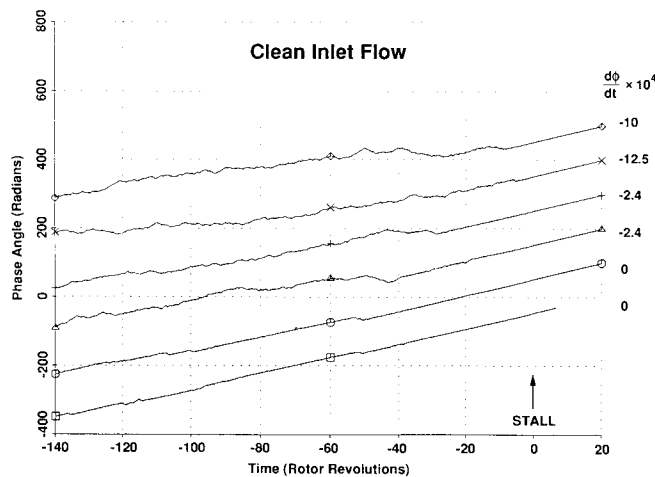
Throttle Transient and Inlet Distortion Effects

The influence of throttle (mass flow) transients and inlet distortion (spatially non-uniform inlet total pressure) is of interest since we know from engine experience that rotating stall is often associated with these phenomena. Experiments were conducted on both the one- and three-stage compressors with qualitatively similar findings.

The throttle transient experiments were conducted at three different throttle rates which varied by a factor of 150 to 1, the fastest corresponding to a flow coefficient range of roughly 0.1 (Fig. 3) per 100 rotor revolutions. Distortion was generated by blocking off 180° of the annulus approximately one compressor diameter upstream of the IGV's, creating a roughly square wave total pressure distortion with an amplitude of 0.5 dynamic head, based on mean velocity. The time-resolved mass flow for these experiments was obtained using the average of the hot wire measurements. The time derivative of the mass flow was obtained by a least-squares fit to the last second of data preceding stall. The absolute uncertainty of these measurements was estimated at 5%.

The prestall behavior of the three-stage compressor with a uniform (Fig. 9) and distorted (Fig. 10) inlet flow was measured at three throttle rates. In both cases, the rotating stall was always preceded by low amplitude waves travelling at constant speed. The prestall duration of these waves is roughly inversely proportional to the throttle rate. This is consistent with the stability model in that the higher the throttle rate, the less time the machine spends at the low flow (ϕ) region of the speedline which has low damping (σ) and, thus, the shorter the period during which the prestall waves can propagate for an appreciable time.

The flow coefficient (ϕ) at which prestall waves are first discerned is shown in Fig. 11 for the single-stage compressor as a function of non-dimensional throttle rate ($d\phi/dt$), where t is measured in rotor revolutions, i.e. t = time/rotor revolution period. The waves appear at nearly the same value of ϕ independent of the throttle rate (over the rates examined, the waves appear slightly later as $d\phi/dt$ increases). The prestall period of constant travelling wave speed (the straight line segments in Figs. 9 and 10) is plotted in Fig. 12 as a function of the throttle rate and exhibits (roughly) a $1/(d\phi/dt)$ dependence.

The effects of inlet distortion are evident in Figs. 9-11. The prestall period at near-zero throttle rate is an order of magnitude smaller with the inlet distortion than without. This behavior is also consistent with a model such as that described by Eq. (1) if we consider that wave propagation velocity and amplitude are functions of the local flow conditions and thus will vary about the annulus in the case of distorted inflow. We infer that the signal processing technique used here (Eq. (2)), which looks only for *sinusoidal*
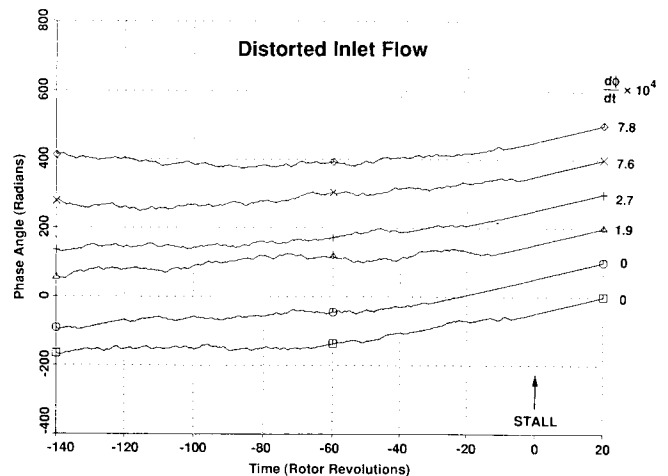

Fig. 9: Phase angle of first harmonic measured on the low speed, three-stage compressor at different throttle rates.
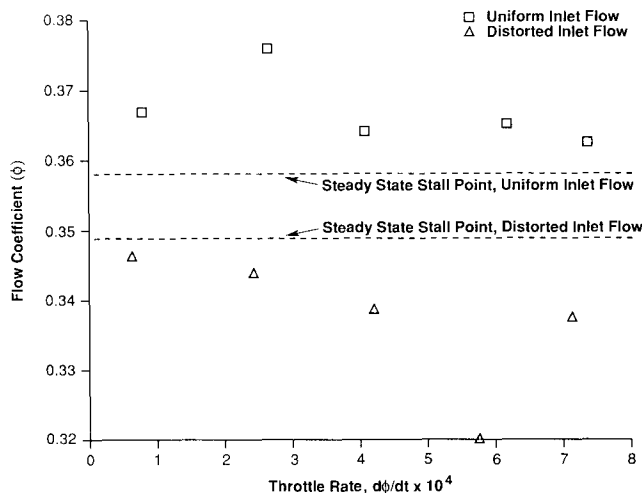

Fig. 10: As Fig. 9, but with inlet distortion.

5

Fig. 11: Flow coefficient (ϕ) at which prestall waves are first discerned in the low speed, single-stage compressor as a function of throttle rate.

Fig. 12: Period during which the prestall wave is discerned as a function of throttle rate.

waves, is not optimal with inlet distortion. Instead, a method based on the true eigenmodes of the system -- and thus independent of wave shape -- should be used. These could be calculated using the procedure outlined by Hynes and Greitzer (1987), but we have not yet taken this step.

Sensor Placement Influence

Data was taken with the circumferential array of sensors at five different axial stations upstream, downstream, and between the blade rows of the single-stage compressor to evaluate the influence of sensor placement on travelling wave detection. The waves were discernible at all axial stations. The amplitude increased as the sensors were moved downstream but so did the noise. This is reflected in Fig. 13, which shows the signal-to-noise ratio, defined as the mean of the amplitude of the first harmonic ($|C_1|$) of the wave divided by the standard deviation. The signal is cleanest upstream of the IGV's.

Disturbance Growth Rate

The general nonlinear model that gives rise to Eq. (1) describes the evolution of the travelling wave system in the compressor and it should be capable of quantitatively predicting the growth of the waves. The inputs required for the calculation are the compressor geometry (lengths, blade stagger angles, etc.) and the steady state compressor characteristic. Comparison of model prediction with experimental measurement for the three-stage low speed compressor (Fig. 14) shows good agreement. (Note that, since the initial conditions for the model are not known, the zero time reference for the data and the calculation are arbitrary.) In our view, this agreement helps establish the validity of the model.

HIGH SPEED COMPRESSOR EXPERIMENTS

The wall static pressure history measured just upstream of the first stage stator in a three-stage high speed compressor with uniform inlet flow during a slow throttle transient is shown in Fig. 15. The data are for eight circumferential locations. The phase speed of the first two spatial harmonics of this data as calculated using Eq. (2) shows that the second harmonic is most readily discerned, Fig. 16. The prestall amplitude [$|C_N|$] is considerably higher for the second harmonic as well. The wave speed is constant for more than 100 rotor revolutions, showing a behavior similar to that of the low speed compressors. Comparison of the phase speed of the second harmonic as measured at the leading edge of each of the three stator rows (Fig. 17) shows the signal to be clearest at the first stage.
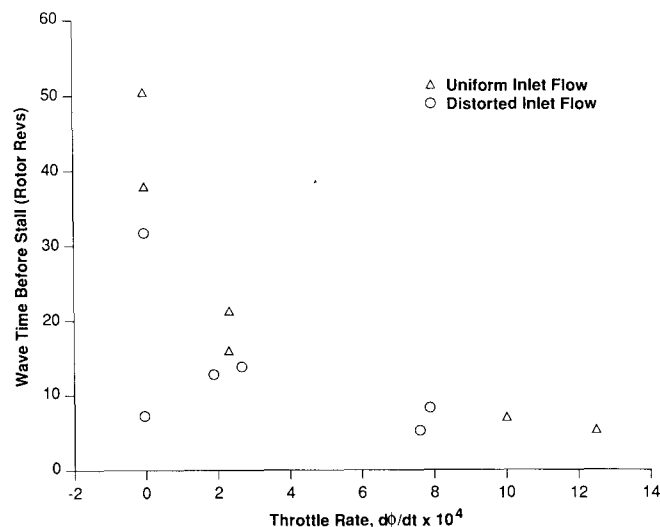
Other measurements and calculations indicate that the first stage stalls first under these flow conditions.

Time history of the wall static pressure on the high speed compressor with a 180° inlet distortion during a slow throttle transient is shown in Fig. 18. Here we see that the prestall disturbance level is not uniform about the circumference. The phase speeds of the first two spatial harmonics of this data are not readily discerned (Fig. 19) except for a short stretch of the second harmonic. The reason for this may be inferred from the time histories in Fig. 18 which show prestall disturbances of relatively high amplitude originating on sensor 7 (low flow region) being strongly attenuated as they move by sensors 6 and 5 (high flow region). Cross-correlations of adjoining sensors were taken which indicated a maximum at a time delay corresponding to 13% of rotor speed. A time history of the maximum value of the cross-correlation between
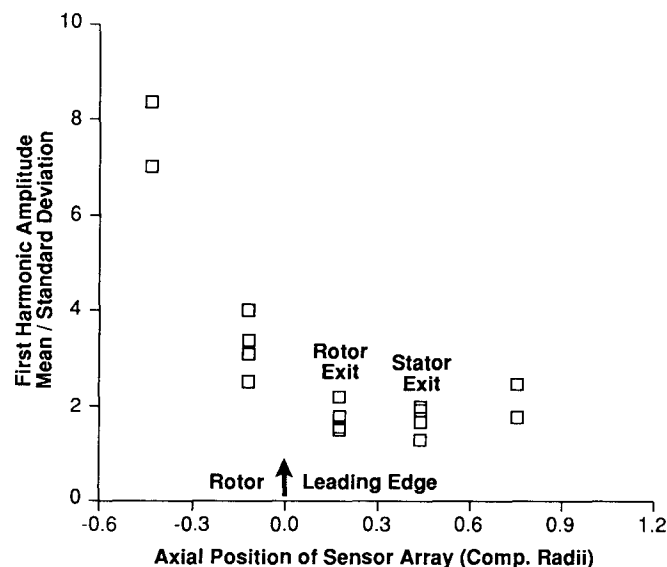

Fig. 13: Signal-to-noise ratio of first Fourier coefficient amplitude measured at various axial stations in the single-stage compressor.
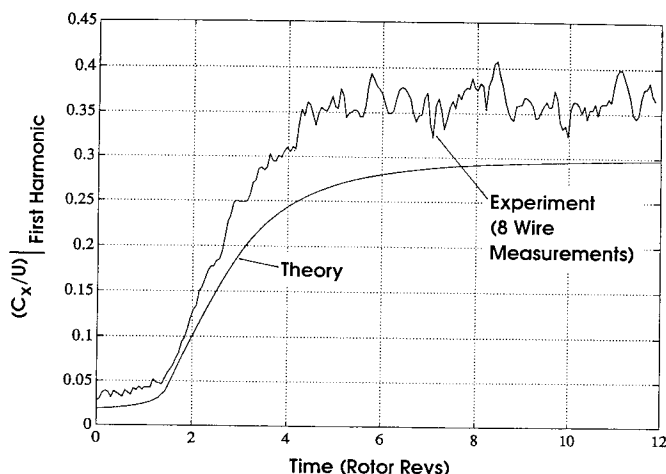
6

Fig. 14: Time evolution of the first harmonic of the axial velocity in the three-stage compressor during the inception of rotating stall.

sensors 0 and 1 shows (Fig. 20) strong correlation for the period (-100 to -140 revs) during which constant phase speed of the second harmonic can be discerned. The correlation increases again as stall is approached.

These high speed data support the view that the distorted compressor acts (crudely) as parallel compressors with wave speed and damping varying about the circumference as a result of the locally varying flow field. The cross-correlations of both high and low speed compressor data show that there is local real-time information available on the instantaneous compressor stability, which may require more sophisticated data processing than represented by Eq. (2).

APPLICATION OF SIGNAL PROCESSING TO COMPRESSOR STABILITY ESTIMATION

We believe that the experimental data presented has verified the applicability of the compressor stability model represented by Eq. (1), at least to the three machines studied. In this view, compressor

stability is directly linked to the growth or decay of the travelling waves and rotating stall is simply the mature form of this wave evolution. The question of stall warning thus becomes one of identification of the waves and estimation of their growth rate. The practical implementation of this approach is complicated by two factors. The first is that, during transients, the growth of the disturbance may not be slow compared to its fundamental period, and this reduces the effectiveness of the more simple time spectra techniques such as fast Fourier transforms (FFT). The second is that the circumferentially nonuniform flowfield of a compressor with inlet distortion means that wave growth and propagation rates are nonuniform about the circumference, reducing the effectiveness of the simple spatial analysis approach of Eq. (2). To extract the maximum information available from the compression system, more sophisticated signal processing is thus required to cope with temporal and spatial variations. In the following sections, we address only the problem of temporal variability, leaving the spatial variation problem to a later time.

As sketched in the Appendix, the wave behavior of Eq. (1) is associated with the temporal behavior of the Fourier modes (a_k) of the velocity potential of the form

$$\frac{da_k}{d\xi}(\xi) = C_k a_k(\xi) \tag{3}$$

which is the description of a first order system in which C is a constant that depends on geometry. Two interrelated approaches can be brought to bear on this system: spectral analysis and system identification techniques.

Spectral Analysis

In its simplest form, spectral analysis can be used to estimate the power spectral density (PSD) of each important spatial harmonic of the flowfield. A peak should be present at the frequency of the travelling waves (20-40% of rotor rotation) with its height being proportional to the power in the wave. Monitoring the time evolution of this peak yields information on the wave growth and thus the compressor stability. This should be a more discerning technique than the simple phase speed plots (as in Figs. 7, 9, 10, and 15), since the phase is driven by the strongest frequency component present in the signal which is not necessarily that of the travelling waves of interest, while the PSD will not be so affected.

The fast Fourier transform (FFT) is often used to calculate PSD's but has two limitations that are important in this application. The first is that the frequency resolution is proportional to the time
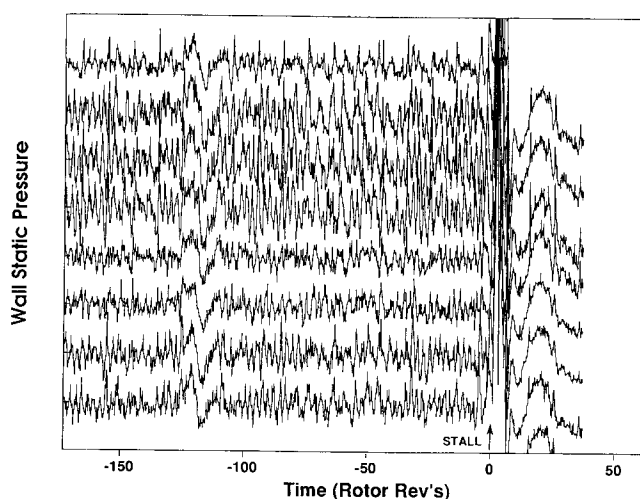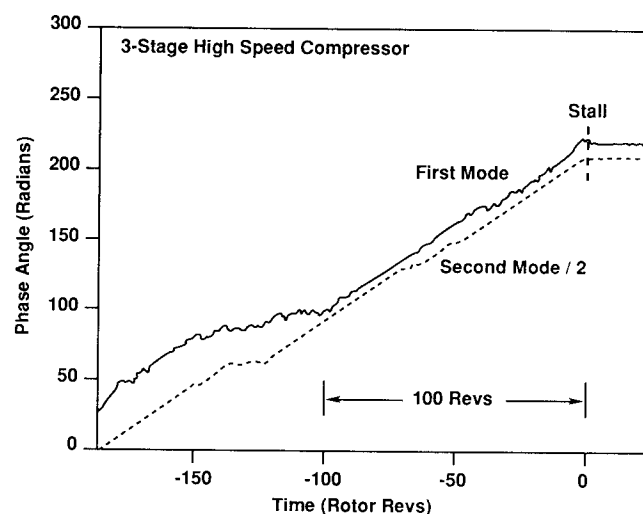

Fig. 15: Time history of 8 wall static pressure transducers located about the circumference ahead of the first stator row in a high speed, three-stage compressor.

Fig. 16: The phase history of the first two spatial harmonics calculated from the high speed compressor data of Fig. 15.

7

interval available for analysis. The second is that the absence of information outside this interval distorts the spectral response. These problems can be particularly troublesome with very short data records and data with time varying spectral content, both of which are present in this application. Other techniques have been developed, however, which largely overcome these problems. The one adopted here is based on the fitting of a linear model to the data (Kay and Marple, 1981) which has the advantage of resolving sharp spectral features from short data records.

The power spectral densities of the first spatial harmonic of the axial velocity before stall in the single-stage and the three-stage low speed compressors are shown in Fig. 21. The travelling wave is readily apparent in both compressors, at 0.24 of rotor frequency for the single-stage and 0.35 for the three-stage. (The three-stage data was low pass filtered to remove the d.c. component; the single-stage data was not.) Figure 21 shows the power spectra at one flow coefficient at one instant of time. The power in the travelling wave (i.e. the height of the peak at the travelling wave frequency of Fig. 21) is plotted in Fig. 22 as a function of flow coefficient. The amplitude of this peak at the travelling wave frequency increases as the flow coefficient is decreased, implying that the power in the waves is related to the compressor stability. Note that the power in this first spatial harmonic is considerably reduced when inlet distortion is present. This is most likely a result of the signal processing technique used here, which was aimed at discerning sinusoidal waveforms travelling about the compressor circumference. The distorted inflow waveforms are not so simple, thus more sophisticated processing techniques may be required. The direct spectral approach lets us identify flow features but does not directly yield information on compressor stability, since the height of the peak is a function both of the damping of the system and the amplitude of the excitation. System identification techniques are of use in this respect.

System Identification

We have a model (Eq. (1)) which we believe to be a relevant description of the physical system, compressor stability. System identification is a technique which allows us to estimate the values of the physical parameters describing the compressor stability by fitting data to the model in real time. A discrete time series y_n can be modelled as the solution of a difference equation

$$y_n = b_1 y_{n-1} + ... + b_p y_{n-p} + v_n \qquad (4)$$

where v_n is a noise term (turbulence, electrical noise, convected

Fig. 18: As Fig. 15, but with inlet distortion.

disturbances, etc.). The p coefficients of b_i in Eq. (4) can be estimated by fitting a pth order linear model to the data. The advantage in this application is that only the parameters need be estimated since the form of the model has been established. Filtering can be used to enhance the results by removing unmodelled dynamics and correlated noise.

The model can be fitted to the data in either the time or frequency domain. The time domain was used here since it is well suited to real-time implementation. Least squares techniques can be used recursively by updating the model parameter estimates for each new data point (Goodwin and Sin, 1984; Friedlander, 1984) and "forgetting" old data to track time varying parameters. We refer the reader to Garnier (1989) for further details.

We rewrite the wave model of Eq. (3) for each spatial harmonic in the form of Eq. (4) as an ordinary differential equation

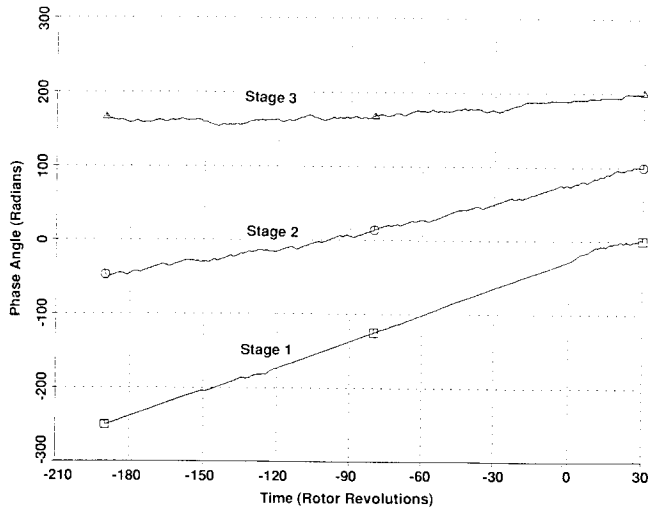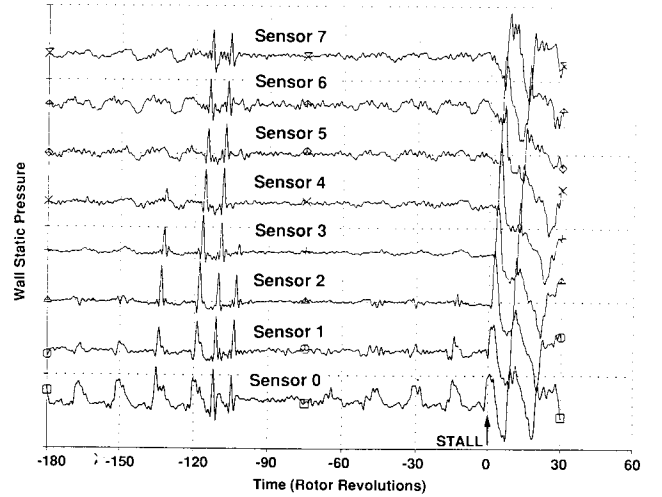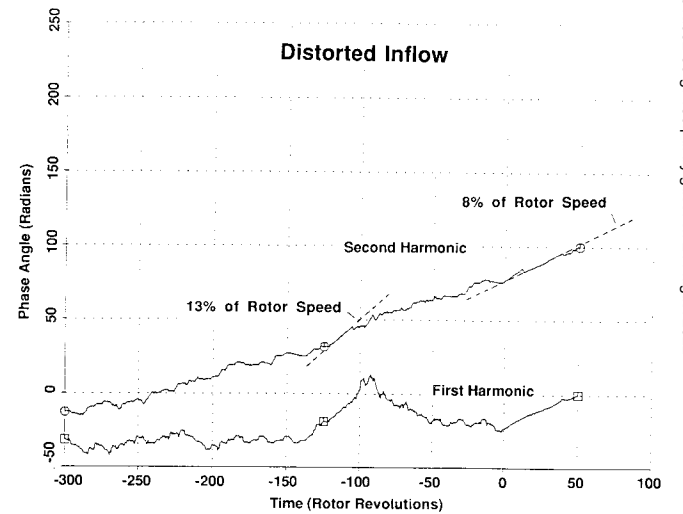$$\frac{dC_{-k}(\xi)}{d\xi} = (\sigma_k - i\omega_k) C_{-k}(\xi) + V(\xi) \qquad (5)$$

Fig. 17: Phase history of first spatial harmonic from measurements taken at the stator leading edges in a high speed, three-stage compressor.

Fig. 19: Phase angle history of the first two spatial harmonics of the high speed compressor with inlet distortion.
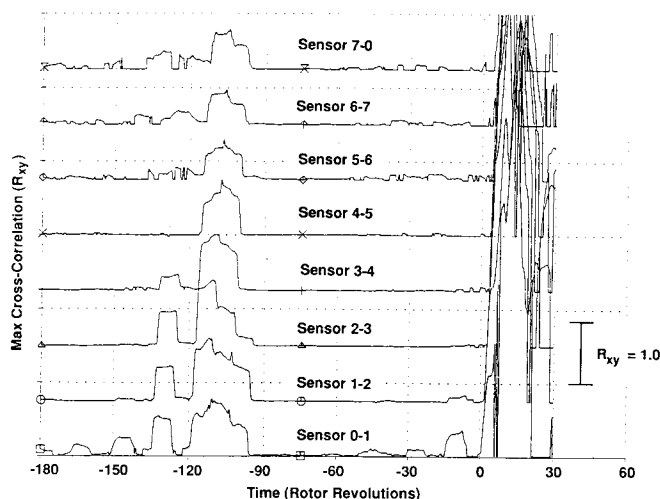
8

Fig. 20: The maximum value of the cross correlation of the adjacent transducers of Fig. 8 in a high speed, three-stage compressor.

where C_{-k} is the harmonic defined by Eq. (2), σ_k the travelling wave damping, ω_k the wave frequency, and $V(\xi)$ the driving noise. In fitting this model to the data at any instant in time, we have estimated the wave damping and frequency for each spatial harmonic. To the degree to which the model is valid, wave damping and compressor stability are equivalent. A real-time estimate of σ is thus an instantaneous measure of the compressor stability.

The fit of Eq. (5) to the power spectral density of the first spatial harmonic of the single-stage low speed compressor is shown in Fig. 23 for undistorted flow and Fig. 24 for distorted inflow. In both cases, the model fits the general shape of the data well. The distorted data shows a peak frequency of -0.3 which is too close to travelling wave frequency to simply filter, so a second order model was employed to account for this peak. All of the distorted inlet data subsequently used a second order model.

The damping coefficient (σ_1) of the first spatial harmonic estimated with this technique from the data is shown as a function of flow coefficient in Fig. 25, with and without inlet distortion. With undistorted inflow, the compressor is stable until the damping approaches zero. With inlet distortion, the damping is greater than for the undistorted case away from stall, but drops much faster with flow coefficient until the machine stalls at a somewhat higher value of σ. The frequency of the first spatial harmonic (ω_1) is the same with and without inlet distortion and independent of flow coefficient. The influence of throttle transients is apparently to steepen the drop in damping with flow coefficient as well as delay the stall to a somewhat lower flow coefficient (Fig. 26). How much of the delay is due to unmodelled inertia effects within the compressor and how much is due to time lags in the algorithm has not been determined.

DISCUSSION -- ENGINEERING USES OF PRESTALL WAVES

As we have demonstrated, the compressor damping can be directly estimated on-line, given sufficient experimental data. The damping is a direct measure of the compressor stability over the period represented by the data and is thus an indication of the likelihood of stall. Whether or not a machine stalls at a given time is determined not just by the system damping, however, but also by the nature and level of the system forcing, which we have not addressed here. The damping by itself, though, is an indication of the susceptibility to the excitation and thus to stall.

One use of this information would be to establish the surge line of a new compressor on the test stand without the necessity of actually stalling the machine. This avoids the requirement to

automatically "dump" the compressor to a higher mass flow each time surge is encountered (necessary to prevent mechanical damage), and can provide a savings in test time. A second possible use is to determine the location within a multistage compressor of the blade row in which the stall starts. The data from the high speed compressor indicated that the waves are most clearly discerned at this axial station.

One of the most intriguing and challenging uses would be as a real-time prestall indicator in an operational engine. The limited data presented herein suggest that sufficient warning time may be available (tens to hundreds of rotor revolutions) for a more or less conventional engine control system to take corrective action (changing fuel flow, nozzle area, vane settings, etc.), thus reducing the surge margin required and the associated penalties. There are many questions which must be examined before the practicality of such a scheme could be established -- not just ones of compressor dynamics as addressed here but also more applied ones such as sensor reliability, computational requirements, system complexity, overall dependability, and cost.

An even more challenging use of these prestall waves is as a control signal for an actively stabilized compressor, one in which external feedback control is used to increase the compressor stability by increasing the wave damping (σ). Epstein, Ffowcs Williams, and Greitzer (1989) first suggested this approach and an ongoing effort was described by Dugundji et al. (1989), where the inlet guide vanes of a single-stage low speed compressor were being "wiggled" to suppress the travelling waves and thus increase the compressor stability.

For any of these applications to become practical, considerably more work than presented here must be done on the sensing and identification of these circumferentially travelling waves. In particular, the sinusoidal nature of the signal processing inherent in Eq. (2) must be relaxed in order to account for more complex flows, such as those with inlet distortion. Algorithm selection and adaptation to minimize the length of time data must be taken to identify the waves is another area where work is needed. We believe
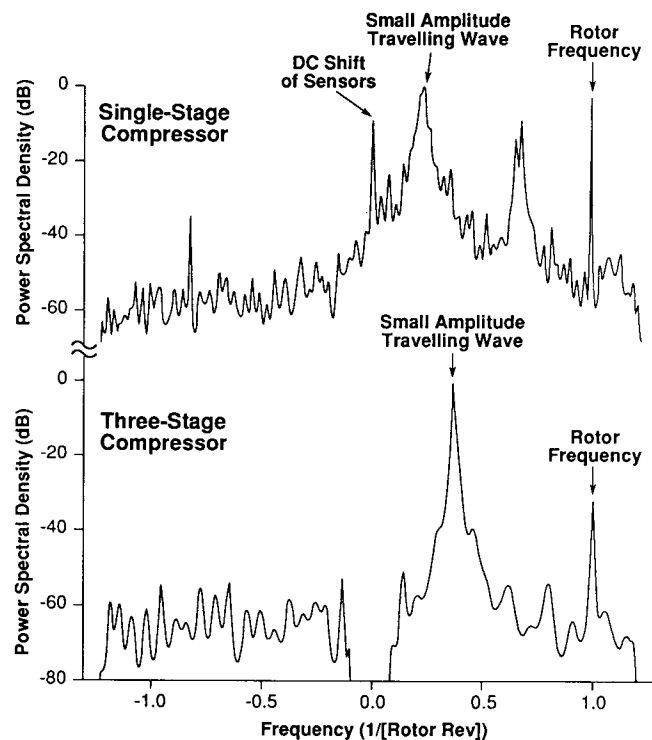

Fig. 21: Power spectral density (PSD) of first spatial harmonic of the axial velocity before stall in two low speed compressors.
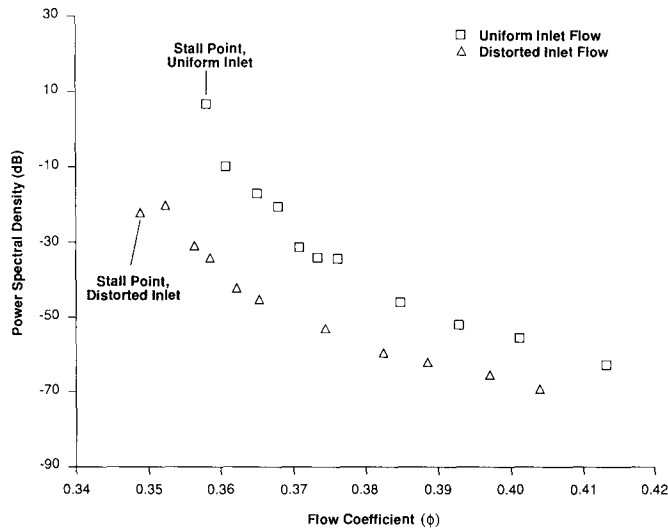
Fig. 22: The peak power of the first spatial harmonic as a function of flow coefficient (φ) on the single-stage, low speed compressor

these extensions of the present work are straightforward, although not necessarily simple. Somewhat more complicated (or at least tedious) is the analytical inclusion of compressibility to accurately model high speed machines (although the high speed data examined to date is quite similar to that from low speed machines).

An extremely fundamental question is how general are the results presented herein -- do some, most, or all compressors exhibit this prestall wave behavior? We make no claims beyond the results for the compressors we have examined. All exhibit similar behavior, behavior in accord with the theoretical models of compression system stability.

We know of no reason why such waves should not exist in all compressors, although we would not be at all surprised if their strength and duration varied to such a degree as to render them very difficult to discern in some machines. Only more data can answer this question.

CONCLUSIONS AND SUMMARY

We have examined the flow in two low speed and one high speed compressor. The experiments in these machines show that:
1. Small amplitude (less than 5% of the stall amplitude) waves can be discerned travelling about the compressor annulus at close to the rotating stall speed for 10-200 rotor revolutions prior to the onset of rotating stall.
2. These waves grow into a fully developed rotating stall without apparent sharp changes in either phase or amplitude.
3. The prestall period during which these waves were discerned varied by a factor of 5 at a single flow condition, apparently stochastically.
4. The behavior was similar in both the high and low speed compressors, except that the first spatial harmonic was the strongest in the low speed machines and the second in the high speed.
5. In multistage compressors, the prestall waves are clearest in the stage which stalls first.
6. Inlet distortion reduces the period during which the prestall waves were discerned, using techniques based on the assumption of sinusoidal waves about the circumference.
7. The data fit the model of Moore and Greitzer, including both the qualitative behavior of the prestall waves and the quantitative prediction of the growth rates.

Overall, we believe that recognition of this wave behavior can be a useful tool in the study of compressor stability. Future work should encompass more sophisticated signal processing to account for distorted inflow, include the effects of compressibility, and extend the experimental work to a larger number of compressors.
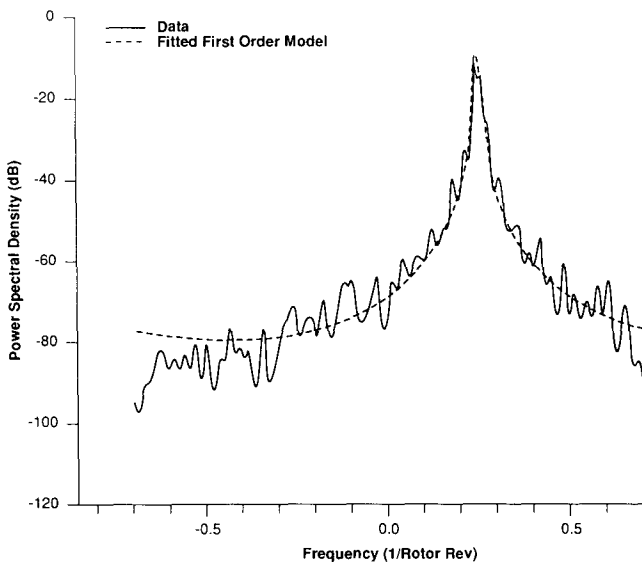
ACKNOWLEDGEMENTS

Fig. 23: Comparison of the linear model and measurement of the power spectral density of the first spatial harmonic on the low speed, single-stage compressor.
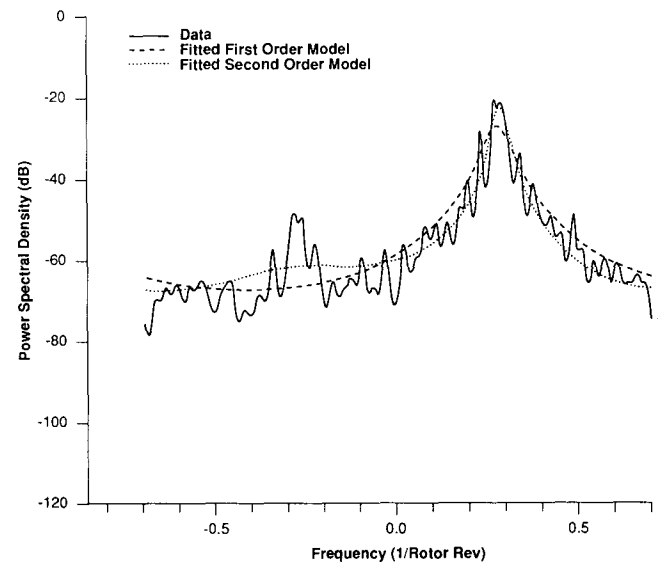

Fig. 24: As Fig. 23, but for second spatial harmonic.

10

REFERENCES

Dugundji, J., Epstein, A.H., Garnier, V., Greitzer, E.M., Guenette, G.R., Paduano, J., Silkowski, P., Simon, J., Valavani, L., 1989, "A Progress Report on Active Control of Flow Instabilities: Rotating Stall Stabilization in Axial Compressors," AIAA Paper 89-1008.

Epstein, A.H., Ffowcs Williams, J.E., Greitzer, E.M., 1989, "Active Suppression of Aerodynamic Instabilities in Turbomachines," Journal of Propulsion and Power, Vol. 5, No. 2, pp. 204-211.

Friedlander, B., 1984, "The Overdetermined Recursive Instrumental Variable Method", IEEE Transactions on Automatic Control, Vol. AC-29, No. 4, pp 353-356.

Gamache, R.N., Greitzer, E.M., 1986, "Reverse Flow in Multistage Axial Compressors", AIAA Paper 86-1747, to appear in Journal of Propulsion and Power, 1990.

Garnier, V., 1989, "Experimental Investigation of Rotating Waves as a Rotating Stall Inception Indication in Compressors," M.S. Thesis, Dept. of Aeronautics and Astronautics, MIT.

Goodwin, G.C., Sin, K.S., 1984, Adaptive Filtering, Prediction and Control, Prentice Hall.

Graupe, D., 1984, Time Series Analysis, Identification and Adaptive Filtering, Robert E. Krieger Publishing Company, Malabar, Florida.

Greitzer, E.M., 1976, "Surge and Rotating Stall in Axial Compressors, Part I: Theoretical Compression System Model", and "Part II: Experimental Results and Comparison with Theory", ASME Journal of Engineering for Gas Turbines and Power.

Greitzer, E.M., Moore, F.K., 1986, "A Theory of Post-Stall Transients in Axial Compressors: Part II - Applications," ASME Journal of Engineering for Gas Turbines and Power, Vol. 108, pp. 231-239.

Hynes, T.P., Greitzer, E.M., 1987, "A Method for Assessing Effects of Circumferential Flow Distortion on Compressor Stability," ASME Journal of Turbomachinery.

Johnson, M.C., Greitzer, E.M., 1987, "Effects of Slotted Hub and Casing Treatments on Compressor Endwall Flowfields", ASME Journal of Turbomachinery, Vol. 109, pp. 380-387.

Kay, S.M., Marple, L.S,, 1981, "Spectrum Analysis - A Modern Perspective", IEEE Proceedings, Vol. 69, No. 11, pp1380-1419.

Lavrich, P.L., 1988, "Time Resolved Measurements of Rotating Stall in Axial Flow Compressors", MIT Gas Turbine Laboratory Report #194.

Lee, N.K.W., 1988, "Effects of Compressor Endwall Suction and Blowing on Stability Enhancement", MIT Gas Turbine Laboratory Report #192.

Ljung, L., Morf, M., Falconer, D., 1978, "Fast Calculations of Gain Matrices for Recursive Estimation Schemes", International Journal of Control, Vol. 27, No. 19, pp 1-19.

Marple, L.S., 1980, "A New Autoregressive Spectrum Analysis Algorithm", IEEE Transactions on Acoustics, Speech, and Signal Processing, Vol. ASSP-28, No. 4, pp 441-454.

McDougall, N.M., 1988, "Stall Inception in Axial Compressors", PhD Thesis, Cambridge University.

McDougall, N.M., Cumpsty, N.A., Hynes, T.P., "Stall Inception in Axial Compressors", submitted to 1989 ASME Gas Turbine Conference.

Moore, F., K., 1983, "A Theory of Rotating Stall of Multistage Axial Compressors: Part I - Small Disturbances", ASME Journal of Engineering for Power.

Moore, F.K., Greitzer, E.M., 1986, "A Theory of Post-Stall Transients in Axial Compressors: Part I - Development of the Equations," ASME Journal of Engineering for Gas Turbines and Power, Vol. 108, pp. 68-76.

APPENDIX A: BRIEF DESCRIPTION OF THE BASIC STALL INCEPTION MODEL

The underlying ideas of stall inception and the approach to the sensing are connected by a simple model which provides a framework to view the phenomenon. Two points concerning rotating stall onset should be stressed at the outset. First, when one considers the actual flow, there are several disparate length scales involved. What is needed is a description of the interaction between flow on the blade element scale (length scales on the order of blade pitch or smaller) and the wave structure in the annulus (flow phenomena with length scale of the radius of the machine). Second, there is strong evidence that the "region" of the blade passage that is responsible for rotating stall is the endwall. Put another way, the
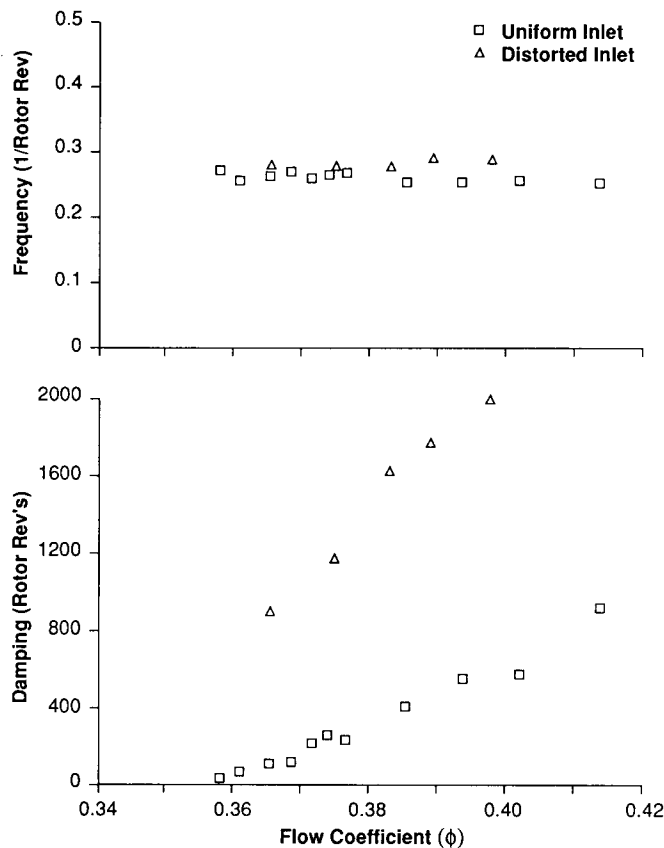

Fig. 25: First spatial harmonic wave damping (σ) and frequency (ω) estimated from the single-stage compressor measurements using parameter identification techniques.
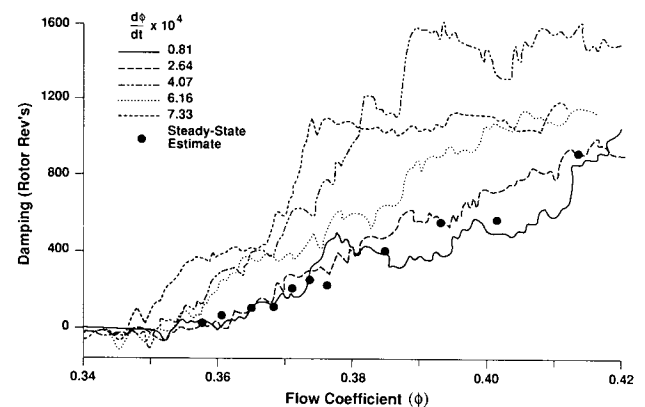

Fig. 26: First spatial harmonic damping, as in Fig. 25, but estimated for various throttle transient rates ($d\phi/dt$).

mechanism of stall is generally not two-dimensional, and treatments that view it as such miss the essential fluid mechanics of the situation.

The model that we use was developed by Moore (1984) for rotating stall and later extended by Moore and Greitzer (1986) to encompass generalized disturbances, i.e. combined rotating stall and surge in multistage machines. Here we examine only onset of the former. In the model, the disturbances upstream and downstream of the compressor are viewed as two-dimensional; this would be expected to be the case in compressors of high hub-tip radius ratio. The blade row description, however, makes use of the measured steady-state compressor pressure rise characteristic, with correction to account for unsteadiness. In a very real sense, then, three-dimensional effects are accounted for because the behavior at the endwalls which can be a strong contributor to the "turn over" in the pressure rise versus flow curve, has been included. Although both the blade row modelling and the coupling between large scale disturbance field and blade element dynamics are crude, the model does appear to contain the necessary elements for a description of the stall process. It is this point, with the simplicity as a secondary issue, that suggests use of such a description in the sensing and control problem.

The derivation of the relevant equations have been given several times elsewhere so that we will only sketch out the steps leading to the equations that we need. The flow fields considered are two-dimensional, inviscid, and incompressible upstream and downstream of the compressor. The flow in these two regions is coupled by three matching conditions across the compressor, two kinematic and one dynamic. With these conditions, representing the modelling of the unsteady and non-axisymmetric compressor performance, we describe the flow in each region as follows.

Upstream Flow Region

Upstream of the compressor the flow is irrotational, and a velocity potential can be used. We express the velocity as a uniform steady flow plus a small asymmetric perturbation which is the gradient of a potential, Φ, satisfying the two-dimensional Laplace equation, with periodic boundary conditions and vanishing far upstream. Φ can thus be expressed in terms of its spatial Fourier coefficients as

$$\Phi(\eta,\theta,\xi) = \sum_{|k|\neq 0} a_k(\xi)\, e^{|k|\eta}\, e^{ik\theta} \tag{A.1}$$

The quantity η is the non-dimensional axial coordinate x/R and ξ is a non-dimensional time, where $\xi = \text{time}\cdot(U/R)$.

Across the Compressor

As stated, there are three matching conditions that are applied across the compressor. The first is that the local axial velocity distribution is the same at all axial stations through the compressor. This approximation is made on the basis of the small opportunity for circumferential redistribution within typical compressors. Order of magnitude arguments imply that it is most correct for disturbances with low order harmonic content, and these are precisely the ones of interest here. Discussion of the assumption can be found in the papers by Dunham (1965) or Stenning (1980).

Explicitly, the matching condition is

$$u_u\,(0,\,\theta,\,\xi) = u_d\,(0,\,\theta,\,\xi)$$

where subscript "u" refers to just upstream and "d" to just downstream of the compressor.

The second matching condition is constant leaving angle at compressor exit. This is also an approximation, but it should be reasonable for the solidities of practical concern.

The last matching condition can be expressed in terms of a relation between the pressure difference across the compressor and the local axial velocity and its derivative. As developed by Moore (1984) (see also Moore and Greitzer, 1986) the matching condition can be written in a linearized form as

$$\left[\frac{\delta P_d - \delta P_{t_u}}{\rho U^2} = \left(\frac{d\psi}{d\phi}\right)\delta\phi - \lambda\frac{\partial\delta\phi}{\partial\theta} - \mu\frac{\partial\delta\phi}{\partial\xi}\right]_{(0,\theta,\xi)} \tag{A.2}$$

The quantity $(d\psi/d\phi)$ is the slope of the steady-state compressor characteristic, and λ and μ are non-dimensional parameters associated with the inertia of the fluid in the compressor blade passages. Their precise values are not critical here since what is of most interest is the general form of the solution, but for reference μ is roughly twice λ and is of order unity.

Downstream Flow Region

The linearized flow field in the downstream region is periodic and obeys the equation

$$\nabla^2\,\delta P_d = 0 \tag{A.3}$$

with the boundary condition far downstream of constant static pressure. The downstream pressure field is thus of the form

$$\delta P_d = \sum P_{n_d}(\xi)\, e^{-|k|\eta + ik\theta} \tag{A.4}$$

Using the linearized forms of the equations of motion in the upstream and downstream region equations, (A.1), (A.2), and (A.4) may be combined into a single equation for $a_k(\xi)$, the Fourier component of the upstream velocity disturbance potential. This is

$$\frac{da_k(\xi)}{d\xi} = \frac{|k|\left|\left(\frac{d\psi_c}{d\phi}\right) - ik\lambda\right|}{(2 + |k|\mu)}\, a_k(\xi) \tag{A.5}$$

If we define

$$\sigma_k = -\left(\frac{d\psi_c}{d\phi}\right)\frac{|k|}{2 + |k|\mu} \tag{A.6}$$

$$\omega_k = k\lambda\,\frac{|k|}{2 + |k|\mu} \tag{A.7}$$

The solution of Eq. (A.5) can be written

$$a_k(\xi) = b_k\, e^{(-\sigma_k - i\omega_k)\xi} \tag{A.8}$$

and thus

$$\Phi = \sum_{|k|\neq 0} b_k\, e^{(|k|\eta - \sigma_k\xi)}\, e^{i(k\theta - \omega_k\xi)} \tag{A.9}$$

As stated in the main text, therefore, the Fourier mode is the product of two exponentials. The term $e^{i(k\theta - \omega_k\xi)}$ represents a travelling wave, with ω_k the wave frequency. The other exponential, $e^{|k|\eta - \sigma_k\xi}$, gives the dependence of the wave amplitude on axial position (η) and time; σ_k is the damping of the wave.